Potential of 'Flat' Fiber Evanescent Wave Spectroscopy to Discriminate Between Normal and Malignant Cells *in vitro*

Z. HAMMODY[1], M. HULEIHEL[2@], A. SALMAN[1], S. ARGOV[3] , R. MOREH[1], A. KATZIR[4] & S. MORDECHAI[1@]

[1] *Department of Physics and the Cancer Research Center, Ben-Gurion University (BGU), Beer-Sheva, 84105, Israel*

[2] *Department of Virology and* Developmental *Genetics, Faculty of Health Sciences, Ben-Gurion University of the Negev, Beer-Sheva, Israel.*

[3] *Department of Pathology, Soroka University Medical Center (SUMC), Beer-Sheva, 84105, Israel*

[4] *School of Physics and Astronomy, Tel Aviv University, Israel*

[@] **Corresponding authors:**

Shaul Mordechai

Tel: +972-8-646 1749; Fax: +972-8-647 2903

E-mail: shaulm@bgu.ac.il

Mahmoud Huleihel

Tel.: +972-8-646-1999; fax: +972-8-647-2970

E-mail: mahmoudh@bgu.ac.il.

Key words: Evanescent wave spectroscopy, infrared microscopy, flat fiber, cell lines, diagnosis.

Abstract

The present study focuses on evaluating the potential of flattened AgClBr fiber optic evanescent wave spectroscopy (FTIR-FEWS) technique for detection and identification of cancer cells *in vitro* using cell culture as a model system. The FTIR-FEWS results are compared to those from FTIR-Microspectroscopy (FTIR-MSP) method extensively used to identify spectral properties of intact cells. Ten different samples of control and malignant cells were measured in parallel by the above two methods.

Our results show a significant similarity between the results obtained by the two methodologies. The absorbance level of Amide I / Amide II, phosphates and carbohydrates were significantly altered in malignant compared to the normal cells using both systems. Thus common biomarkers such as Amide I / Amide II, phosphate and carbohydrate levels can be derived to discern between normal and cancer cells. However, marked differences are also noted between the two methodologies in the protein bands due to CH_3 bending vibration (1480-1350 cm^{-1}). The spectral differences may be attributed to the variation in the penetration depth of the two methodologies. The use of flattened fiber rather than the standard cylindrical fiber has several practical advantages and is considered as an important step towards *in-vivo* measurements in real time, such as that of skin nevi and melanoma using special designs of fiber optic based sensors.

Introduction

Cancer is considered today as one of the leading causes for death worldwide. It may be induced by a variety of factors, including carcinogens (Buttel, 2000), radiation, genetic factors and /or DNA and RNA viruses (Persons et al., 1989; Buttel, 2000; Resonberg & Jolicoeur, 1997). Early detection of cancer is critical for successful therapy and chances for full recovery in many types of cancer.

Infrared (IR) spectroscopy is a reagent free, harmless methodology that has been applied for identifying various biomolecular components of intact cells (Mantch & Chapman, 1996; Diem et al., 1999). One of the most promising fields of application of FTIR spectroscopy is in biomedicine, particularly in the detection and monitoring of characteristic changes in molecular compositions and structures that accompany the transformation from a normal to a cancerous state (Andrus & Strickland, 1998; Salman et al., 2001). Therefore, such technique can be developed into a powerful diagnostic tool of very early stages of cancers which may not be observed by standard diagnostic methods.

FTIR spectroscopy investigations of lung (Wang et al.,1997), breast (Gao et al., 1999), cervical (Regas et al., 2000), prostate (Malins et al., 1997), skin (Garcia et al., 2004) and colon (Salman et al., 2001) cancers have been shown to correlate well with the diagnoses of pathologists. However, the potential of FTIR-FEWS has not been studied in details *in-vitro* or *in-vivo*. FTIR-FEWS technique is based on the phenomenon of attenuated total reflection (ATR) and on IR transparent optical fibers which serve as a wave guide for the IR light. This technique was found useful in industrial (Bindig et al., 2001; Raichlin et al., 2004) and biomedical fields (Ring et al., 2006). In the medical fields FEWS was studied for the detection of cancerous tissues (Ring et al., 2006; Goldberg et al., 2004),

but in most cases the obtained results were not conclusive due to low signal to noise ratio compared to results obtained in transmission mode using an IR microscope (Rave & Katzir, 2002).

In the present study, we evaluate the potential of flat fiber evanescent wave spectroscopy (FTIR-FEWS) by comparing the deduced results with the microscopic data measured on the same samples. The flat fibers were found to give a better signal to noise ratio compared to the cylindrical fibers (Raichlin et al., 2003). The flattened fiber FEWS technique show marked spectral differences between the transformed and the normal cells. While the results from the microscopic and FEWS show similar trends, some marked spectral differences are also noted. These differences may be attributed to the variation in the penetration depth in the sample probed by transmission versus total reflection methodologies.

Materials and Methods

Cells and viruses. Cells were cultured in Dulbecco's modified Eagle's medium (DMEM) containing 10% fetal calf serum (FCS), 1% glutamine, 50 U/ml penicillin, and 50 µg/ml streptomycin, at 37°C in a humidified air containing 5% CO_2.

The cells used in this study are mouse fibroblast cell line (NIH/3T3) and NIH/3T3 cells which were fully transformed to malignant cells by infection with the murine sarcoma retrovirus (MuSV). Clone 124 of TB cells chronically releasing Moloney MuSV-124 was used to prepare the appropriate virus stock. NIH/ 3T3 and clone 124 of TB cells were obtained from the American Type Culture Collection (ATCC).

Cell proliferation. Cells, seeded at a concentration of 0.2×10^6 cells per well in 24 wells plate, were incubated for five days at 37°C in RPMI medium supplemented with 10%

newborn calf serum (NBCS) and the antibiotics penicillin, streptomycin and neomycin. Each day, the cells were examined for morphological changes, and the number of cells was counted with a hemacytometer.

Cell infection and determination of cell transformation. A monolayer of cells grown in a 9-cm^2 tissue culture plate was treated with 8 μg/ml of polybrene (a cationic polymer required for neutralizing the negative charge of the cell membrane) for 24h before infection with the virus. Excess polybrene was then removed, and the cells were incubated at 37°C for 2 h with the infecting virus (MuSV-124) at various concentrations in RPMI medium containing 2% of NBCS. The nonabsorbed virus particles were removed, fresh medium containing 2% NBCS was added, and the monolayers were incubated at 37°C. After two to three days, the cell cultures were examined for the appearance of malignant transformed cells by microscopic observation and by the soft agar assay.

Soft agar assay. A mixture of 25% of 2% Bacto agar, 25% of RPMI × 2 (concentrated medium), 20% of NBCS and 30% of RPMI was prepared, and 4 ml of this mixture was poured into each of a number of 50-mm petri dishes. The mixture was left to polymerize at room temperature for about 30 min. This procedure gave a solid agar (0.5%) layer. Onto each solid layer was poured 1 ml of 0.36% agar containing the test cells. This upper layer was prepared by mixing of 18% of 2% Bacto agar, 18% of RPMI × 2, 20% of NBCS and 44% of RPMI. About 10^5 cells were added to each plate. The plates were left at room temperature for about 20 min and then incubated at 37°C in humidified air containing 5% CO_2 for about 14 days. At the end of the incubation period, colonies of transformed cells were counted under a light microscope.

Preparation of samples. We placed the samples at the flat part on the AgBrCl fiber, which is highly transparent to IR radiation. Normal cells from passage 3-5 or transformed cells (from a fully transformed cell culture) were washed twice with saline and picked up from the tissue culture plates after treatment with trypsin (0.25%) for 1 min. The cells were pelted by centrifugation at 1000 rpm for 5 min. Each pellet was washed twice with saline and resuspended in 100 µl of saline. The number of cells was counted with hematocytometer, and all tested samples were pelted again and resuspended in an appropriate volume of saline to give a concentration of 1000 cells/µl. A drop of 1 µl of each sample was placed on a certain area on the zinc sellenide crystal, air dried for 4h and examined by FTIR microscopy. The radius of such 1-µl drop was about 1 mm.

FTIR-Microscopy (MSP): The FTIR microscopy measurements were performed in transmission mode using FTIR microscope (Bruker IRScope II) coupled to an FTIR spectrometer (BRUKER EQUINOX model 55, OPUS software). A liquid nitrogen-cooled MCT detector was used.

FTIR-Fiber-optic Evanescent Wave Spectroscopy (FEWS): This technique is based on the phenomenon of attenuated total reflection. Our FEWS system is based on a modified FTIR-spectrometer (Bruker, Vector 22; Karlsruhe, Germany). A coupling unit was inserted inside the compartment sample cell which made it possible to connect a flexible $AgBr_{0.5}Cl_{0.5}$ flat fiber to the spectrometer. IR radiation emitted from the source of the spectrometer was focused on the fiber using a ZnSe lens, and the radiation emitted from the fiber was directed onto a cooled IR MCT detector. The fiber length was 11 cm and its diameter was 0.9 mm, the flat part length was 4.5 cm and its thickness D= 0.15 mm. In an

earlier study it was found that the absorbance signal in the fiber was inversely proportional to the thickness (D) of its planar (flattened) part (Raichlin et al., 2003). Figure 1c shows the flat fiber used in our measurement with the sample that was placed on its flat part. The evanescent wave propagates by a series of total internal reflections at the wave guide sample interface. Fig. 1d illustrates this phenomenon at the interface between the two media: a wave guide (medium 1) and a sample (medium 2). The sample composed of normal or transformed intact cells is nearly circular with a diameter of 4.5 mm. It is possible to evaluate the penetration depth of the IR radiation using the relation from Maxwell equations (Harrick, 1979)

$$d = \frac{\lambda_1}{2\pi\sqrt{\sin^2\psi - n_{21}^2}}$$

$\lambda_1 = \frac{\lambda}{n_1}$, λ is the wavelength in air, $n_{21} = \frac{n_2}{n_1}$ where n_1 and n_2 are the refractive indices of the fiber and the sample respectively and ψ is the incident angle at the contact surface. Assuming that n_1 =2.1 (Paiss et al., 1993), n_2 =1.35 (Li & Xie, 1996) and ψ is limited by the critical angle. For example at λ =10.8 μm (~ 925 cm^{-1}) and ψ = 45° we obtain d ≈ 2 μm. The average penetration depth (over all internal reflection angles) is between 2-5 μm in the IR region 5.5-11 μm (Bunganaen & Lamb, 2005).

The spectra were taken in the 600-4000 cm^{-1} mid-IR range in parallel, using the same cell stocks for better and accurate comparison between the two experimental systems. The spectra were averaged over 128 scans to increase the signal to noise ratio (SNR). The SNR obtained in the microscopic data was better than 700 and for FTIR- FEWS it was better than 500. The spectral resolution was set at 4 cm^{-1}.

Baseline correction and normalization were performed for all the spectra using the rubber band method in OPUS software. For the construction of the baseline, each spectrum was divided up into 64 segments of equal size. In each spectral range, the minimum y-value was determined. The baseline was then created by connecting the minima with straight polynomial lines. Starting from "below", a rubber band stretched over this curve constituted the baseline. All the spectra had been arbitrarily normalized to 2 at the Amide I (1649 cm^{-1}). Additional normalization methods were tested (such as Amide II and vector normalization) and gave comparable results. Peak positions were determined using the second derivative method using OPUS software.

In the case of FTIR-MSP, the microscopic aperture used was 100 μm, to obtain good signal/noise ratio. For each cell type, the spectrum was taken as the average of five different measurements at various sites on the sample. The experiments with each cell type were repeated five times for quality verification and statistical analysis. No significant differences were observed in the spectra taken from various sites (SD less than 0.005) in the microscopic measurements. Similarly, in the FTIR-FEWS, repeated measurements gave highly reproducible data.

Results

Normal and Malignant Cell Characteristics

Normal fibroblasts (NIH/3T3) and malignant cells transformed by infection with the retrovirus MuSV were used in this study. NIH/3T3 cells appear as flat cells under an inverted light microscope (Fig. 1a) and were unable to grow on soft agar. When NIH/3T3 cells were infected by MuSV, transformed cells with a highly refractive shape were detected growing randomly in a criss-cross fashion configuration (Fig. 1b). These

cells labeled NIH /MuSV were able to grow on soft agar and to produce large colonies within 5-10 days. NIH/3T3 cells are replicating slower in culture compared to malignant cells and could not survive in very high densities of cell culture.

When 5 x 10^6 transformed cells were injected subcutaneously to newborn mice, only malignant cells were able to produce tumors 2 weeks after injection, while the normal NIH/3T3 cell line were not able produce such tumors (data not shown). These two highly different cell characteristic are most suitable for the present study since they have very different morphology when seeded on the flat fiber.

FTIR-MSP and FEWS Spectra of Normal and Malignant cells

Normal fibroblasts (NIH/3T3) and malignant cells (NIH/MuSV) transformed by infection with the MuSV retrovirus were examined by FTIR-MSP and FTIR-FEWS. Typical spectra of FTIR-MSP and FTIR-FEWS for both cell types in the region 800-1800 cm^{-1} are presented in Fig. 2a and 2b respectively. The prominent spectral bands, well characterized by FTIR-MSP are also observed in FTIR-FEWS (Amide I & II, carbohydrate, phosphates and lipids regions). It can be seen that the NIH/3T3 spectra had higher absorbance intensity in most of the spectral regions compared to NIH/MuSV after normalizing to the amide I band. However, a closer look shows also some marked differences between the spectra obtained by the two methods, such as: (1) the protein bands which are associated with the symmetric and asymmetric CH_3 bending (1350-1480 cm^{-1} region), shown as insets in Fig. 2a and Fig. 2b; (2) Amide I and Amide II band widths; (3) a shoulder which appears in FEWS at 1740 cm^{-1} is not seen in the microscopic data; (4) a triplet structure at 1120, 1081 and 1045 cm^{-1} in the microscopic

spectrum (mostly due to glycogen) is hardly observable in the fiber optic set up where only the band at 1081 cm^{-1} is clearly seen.

The differences between the two methodologies might arise from the intrinsic difference in the sampling since in FTIR-FEWS reflection method, the IR radiation does not penetrate throughout the entire cell thickness, but samples only about few microns deep through the cell membrane while in FTIR-MSP, the IR radiation penetrates through the entire cell volume.

Spectral Biomarkers for Discrimination between Normal and Malignant Cells

Amide I /Amide II ratio is quantified as the ratio of the integrated absorption of Amide I and Amide II (1750-1590 cm^{-1}, 1590-1480 cm^{-1}). This ratio is considered as a good indicator for the DNA absorbance variation (Benedetti et al., 1997; Gasparri & Muzio, 2003). Its value is close to unity for RBCs (red blood cells) which have no nuclei and any deviation from this value is considered as an indication of cellular DNA absorption. The results presented in Fig. 3a & b show the Amide I / Amide II ratios for the transformed cells compared to control cells obtained by both systems. The FTIR microscopic results show a significant difference in this ratio for NIH/3T3 and NIH/MuSV. However, this difference between normal and transformed cells become smaller or diminished (in some cases) in FEWS. As a result of these variations only 80% separation between normal and malignant cells was achieved using FEWS compared to 100% separation obtained by MSP (Fig. 3a and 3b). Fig. 3c shows a comparison for the control NIH/3T3 cells using both systems. Note that the ratio Amide I / Amide II is consistently higher in MSP compared to FEWS.

Quantification of phosphate metabolites, which are composed of energy yielding molecules and nucleic acids, provide a clue on the various states of the cell (Yang at al. 1995). The phosphate content has been calculated by measuring the integrated area of phosphate symmetric (990-1145 cm^{-1}) and asymmetric (1190-1275 cm^{-1}) bands for the control and transformed cells. The phosphate content is significantly higher in controls relative to the transformed cells. While this phenomenon is enhanced in the MSP measurements (Fig. 4a), it can still be seen in the FEWS data (Fig. 4b).

The band at 1045 cm^{-1} (Fig. 2) is attributed to the vibrational frequency of -CH_2OH groups and the C-O stretching frequencies coupled with C-O bending frequencies of the C-OH groups of carbohydrates (including glucose, glycogen, etc.) (Salman et al., 2001). The ratio of the integrated absorbance at 1045 cm^{-1} to that at 1545 cm^{-1} provides an estimate of the carbohydrate absorption (Parker 1971). Our calculations presented in Fig. 5 (a & b) indicate that this ratio is lower in malignant NIH / MuSV cells compared to normal (NIH/3T3) cells. Again the potential of discrimination between normal and malignant cells according to this ratio is superior in MSP (100%) compared to FEWS (80%).

The absorbance of the symmetric and antisymmetric bendings of CH_3 vibration (calculated as the integrated absorbance at 1480-1350 cm^{-1}) per Amide II (Hydrocarbon ratio) is reported to be due to membrane protein bands contribution (Wang et al., 1997; Ramesh et al., 2001). The ratio of hydrocarbon obtained by FTIR-MSP and FTIR-FEWS techniques is presented in Fig. 6. The average values are represented by the corresponding dash / dotted bands which give for control (1.59 ± 0.16) and malignant

cells (2.01 ± 0.17). Such behavior would be expected based on the intrinsic differences between the two sampling methodologies as discussed later.

Table I summarizes the results of a t-Test performed on some of the biomarkers derived from the absorption spectra. The statistical analysis shows that there are significant differences in the spectral signature of the control and transformed cells with respect to three biomarkers in MSP (Amide I /Amide II, phosphate and carbohydrate level) and one biomarker in FEWS (carbohydrate level). It can be seen from this Table that the phosphate level (shadowed) is among the best quantitative biological markers which may be successfully utilized to discern malignant and normal cells in both the microscopic and the fiber optic based systems. It is also evident (Table 1) that the microscopic data is superior to the fiber optic sensor data with respect to all biomarkers in the distinction between the transformed and control cells.

Discussion

FTIR spectroscopy is considered as a promising technique for detection and identification of malignant cells and tissues (Haaland et al., 1997; Huleihel et al. ,2001). Various regions in the mid IR spectra have shown impressive diagnostic features (Benedetti et al,. 1997; Ramesh et al., 2001; Cohanford & Rigas, 1998). In the present study we examined the potential of flat FTIR-FEWS spectroscopy for identification of malignant cells in culture *(in vitro)* as a first step toward future development of a unique technique for *in-vivo* diagnosis of malignancy. Although circular fibers were used previously in FEWS systems for the detection of malignant tissues, their performance was not conclusive due to the small contact surface area with the tissue (Goldberg et al. 2004), yielding low SNR

spectra. In this study we used flattened fiber, D = 150 μm thick, with large contact area between the waveguide sensor and the intact cell. The use of flattened fiber gives an improved SNR compared to cylindrical fibers. It was found that the absorption signal was proportional to 1/D, thus a small thickness of D= 150μm was found optimal and practical to handle (Raichlin et al., 2003).

Cell lines are considered as an ideal model for evaluation of the potential of this technique for detection of molecular cell structure, since they are homogeneous and easy to control various parameters affecting their growth and malignant transformation.

As a control to the FEWS data all samples were examined also by FTIR-MSP. In both methods, our results show that the absorbance of control cells differ than the malignant cells. Various biomarkers such as Amide I /Amide II ratio, carbohydrate and phosphate levels were calculated and found to be similar in their trends in both methodologies. These parameters (Amide I /Amide II ratio, carbohydrate and phosphate levels) were higher for control cells compared to the transformed cells. These results are in agreement with findings obtained previously utilizing FTIR spectroscopy for detection and identification of malignant cells and tissues (Huleihel et al., 2001; Ramesh et al., 2001; Gasparri & Muzio, 2003; Yang at el., 1995). The higher values of these parameters in the control compared to the malignant cells can be explained as follows: (i) Difference in cell volume. It is known that malignant cells have larger cell volume than the normal cells (Ramesh et al., 2001) giving a lower concentration of cellular key chemical groups. (ii) High metabolic activity of the malignant cells in comparison to the normal cells.

The main differences between FTIR-MSP and FTIR-FEWS systems are outlined in Fig. 3c in the Amide I / Amide II ratio. The Amide I / Amide II ratio is consistently lower in

FEWS compared to the microscopic data. This may arise from the lower DNA content probed in the fiber optic system due to the smaller penetration depth of the evanescent waves. An opposite trend is observed for the phosphate (Fig. 4a and 4b) where the fiber optic phosphate content is higher than the microscopic. This feature may arise due to the larger quantity of phosphorylated proteins found in the cell membrane (accessible in FEWS). The average phosphate values for NIH/3T3 and NIH/MuSV (dash blue and red lines respectively in Fig. 4a and Fig. 4b) indicate that for both cell types the FEWS values are higher than the MSP. Similar phenomena are observed also for the carbohydrate content (Fig. 5a and 5b). It is clear from the data presented in Fig. 6 that the CH_3 hydrocarbon level is higher in FEWS compared to the microscopic system for both cell types. This is because the hydrocarbon is present in larger amounts in the cytoplasm (Wang et al., 1997; Ramesh et al., 2001) and thus is accessible within the penetrating IR in the FEWS system. In FEWS there is no limitation on the sample thickness but the penetration depth of the radiation is limited.

Conclusions

Our comparative study of Flat FEWS and FTIR-microscopy indicate the potential of FEWS technique to detect and identify malignant cell in culture. The results presented in this study are highly important and could be considered as a promising step towards the development of flat FEWS-FTIR technique using special designs of fiber optic sensors for the detection and identification of malignant cells and tissues *in vivo*. While FTIR-Microscopy is most suitable for *ex-vivo* and *in-virto* studies of biopsies and cells, the FEWS system has a potential role for *in-vivo* and *in-situ* diagnosis.

Acknowledgements:

The authors acknowledge the Israel Science Foundation (ISF Grant No: 788/01) for the financial assistance in carrying out this work. We thank Y. Raichlin and R. Schneider for their help during experimental setup and data collection.

References

1. Butel, J.S. (2000) Viral carcinogenesis: revelation of molecular mechanisms and etiology of human disease. *Carcinogenesis*, 21, 405-426.

2. Persons, D.A., Schek, N., Hall, B.L.& Finn O.J. (1989) Increased expression of glycosis-associated genes in oncogene transformed and growth-associated states. *Mol Carcinog*, 2, 88-94.

3. Rosenberg, N. & Jolicoeur, P. (1997) Retroviral pathogenesis In: Coffin JM, Hughes SH, Varmus HE (eds) Retroviruses. Cold Spring Harbor Laboratory Press, Cold Spring Harbor, NY, 475-485.

4. Mantsch, H.H, Chapman, D. (1996) Infrared Spectroscopy of Biomolecules, John Wiley, N.Y.

5. Diem, M., Boydston-White, S. & Chiriboga, L. (1999) Infrared spectroscopy of cells and tissues: Shining light onto a novel subject. *Applied Spectroscopy*. 53, 148-161.

6. Andrus, P.G. & Strickland, R.D (1998) Cancer grading by Fourier transform infrared spectroscopy. *Biospectroscopy* 4, 37-46.

7. Salman, A., Argov, S., Jagannathan, R., Goldstein, J., Igor, S., Guterman, H.& Mordechai, S. (2001) FTIR microscopic characterization of normal and malignant human colonic tissues. *Cell. Mol. Biol (Nosiy-le-grand)* 47, 159-166.

8. Wang, H.P., Wang, H.C. & Huang, Y.J. (1997) Microscopic FTIR studies of lung cancer cells in pleural fluid. *Sci. Total. Environ* 204, 283-287.

9. Gao, T., Feng, J. & Ci, Y. (1999) Human breast carcinomal tissues display distinctive FTIR spectra: implication for the histological characterization of carcinomas. *Anal. Cell. Pathol*. 18, 87-93.

10. Rigas, B., Guardia, K., Qiao, L., Bhandare, P.S., Caputo, T. & Cohenford, M.A. (2000) Infrared spectroscopic study of cervical smears in patients with HIV: implications for cervical carcinogenesis. *J. Lab. Clin. Med*. 35, 26-31.

11. Malins, D.C., Polissar, N.L. & Gunselman, S.J. (1997) Models of DNA structure achieve almost perfect discrimination between normal prostate, benign prostatic hyperplasia (BPH), and adenocarcinoma and have a high potential for predicting BPH and prostate cancer. *Proc. Natl. Acad. Sci USA*, 94, 259-264.

12. Ring, A., Schreiner, V., Wenk, H., Wittern, K., Kupper, L. & Kenhane, R. (2006) Mid-infrared spectroscopy on skin using a silver halide fiber probe in vivo. *Skin research and Technology,* 12, 18-23.

13. Bindig, U., Meinke, M., Gersonde, I., Spector, O., Vasserman, I., Katzir, A. & Muller, G. (2001) IR-biosensor: flat silver halide fiber for bio-medical sensing. Sensor and Actuators *B74*, 37-46.

14. Rave, E. & Katzir, A. (2002) Ordered bundles of infrared transmitting silver halide fibers: attenuation, resolution and crosstalk in log and flexible bundles. *Opt. Eng.,* 41, 1467-1468.

15. Raichlin, Y., Fel, L. & Katzir, A. (2003) Evanescent-wave infrared spectroscopy with flattened fibers as sensing elements. *OPTICS LETTERS*, 28, 2297-2299.

16. Harrick, N.J. (1979) Principles of Internal Reflection Spectroscopy," Chap. 2 in: *Internal reflection spectroscopy*,13-66, Harrick Scientific Corporation, Ossining, New York.

17. Paiss, I., Bunimovich, D., & Katzir, A. (1993) Evanescent-Wave Infrared Spectroscopy of Solid Materials using Deformable Silver-Halide Optical Fibers. *Appl. Opt*., 32, 5867-5871.

18. Li, H. & Xie, S. (1996) Measurement Method of the Refractive Index of Biotissue by Total Internal Reflection. *Appl. Opt.,* 35**,** 1793–95.

19. Bunganaen, Y. & Lamb, W. (2005) An Optical fiber Technique for Measuring Optical Absorption by Chromophores in the Presence of Scattering Particles. J. *of Physics,* 15, 67-73.

20. Benedetti, E., Bramanti, E., Papineschi, F.& Rossi, I. (1997) Determination of the relative amount of nucleic acids and proteins in leukemic and normal lymphocytes by means of FT-IR microspectroscopy. *Appl Spectrosc.,* 51, 792-797.

21. Gasparri, F. & Muzio, M. (2003) Monitoring of apoptosis of HL60 cells by Fourier-transform infrared spectroscopy. *Biochem. J.*, 369, 239-248.

22. Yang, D., Castro, D.J, El-Sayed, I.H., El-Sayed, M.A., Saxton, R.E. & Zhang, N.Y. (1995) A Fourier-transform infrared spectroscopic comparison of cultured human fibroblast and fibrosarcoma cells: a new method for detection of malignancies. *J. Clin. Laser. Med. Surg.*, 13, 55-59.

23. Parker, F.S., (1971) Application of infrared spectroscopy in biochemistry, *biology and medicine. Plenum press*, NY.

24. Wang, J., Chi, C.& Lin, S. (1997) Conformation changes in gastric carcinoma cell membrane protein correlated to cell viability after treatment with adamantly maleimide. *Anticancer Res.*, 17, 3473-3478.

25. Jagannathan, R., Salman, A., Hammody, Z., Cohen, B., Gopas, J., Grossman, N.& Mordechai, S. (2001) FTIR microscopic studies on normal and H-Ras oncogene transfected cultured mouse fibroblasts. *Eur. Biophysics.* 30, 250-255.

26. Haaland, D.M., Jones, H.D.T. & Thomas, E.V. (1997) Multivariate classification of the infrared spectra of cell and tissue samples. *Appl. Spectros.,* 51,340-345.

27. Huleihel, M., Salman, A., Erukhimovitch, V., Jagannathan, R., Hammody, Z.& Mordechai, S. (2001) Novel optical method for study of viral carcinogenesis in vitro. *J. Biochem Biophys Methods*., 50, 111-121.

28. Cohenford, M.A. & Rigas, B. (1998) Cytologically normal cells from neoplastic cervical samples display extensive structural abnormalities on IR spectroscopy: implications for tumor biology. *Proc. Natl. Acad. Sci USA,* 95, 15327-15332.

29. Goldberg, I., Shushan, A., Brenner, S., Nadler, B., Raichlin, Y., Shulzinger, E., Gerber, L.& Katzir, A. (2004) Infrared fiber optic spectroscopy: a novel tool for skin diagnosis", Photons Plus Ultrasound: Imaging and Sensing. Edited by Oraevsky, Alexander A.; Wang, Lihong *V. Proceedings of the SPIE*, 5321, 44-50.

Figure Captions

Figure 1: **a**. NIH/3T3 cell morphology used in the present study under an inverted light microscope. **b**. Transformed NIH/3T3 cells after complete infection by MuSV. **c**. Flat fiber used in our measurements with cells placed on the flattened fiber. **d**. Expanded schematic cross section of the flat fiber waveguide illustrating the total internal reflection and the penetration of the evanescent waves in the interface between the waveguide (medium 1) and the sample (medium 2).

Figure 2: Typical spectra of FTIR-MSP (a) and FTIR-FEWS (b) for NIH/3T3 and NIH/ MuSV in the region 800-1800 cm^{-1}. The insets show the expanded region (shadowed) at 1350-1480 cm^{-1}.

Figure 3: Amide I / Amide II calculated as the ratio of the integrated absorbance of Amide I (1750-1590 cm^{-1}), and Amide II (1590-1480 cm^{-1}) using: (a) FTIR-MSP and (b) FTIR-FEWS. (c) Comparison between the microscopic (MSP) and the flattened fiber optic data (FEWS) for NIH/3T3.

Figure 4: Phosphate levels calculated by the integrated absorbance of phosphate symmetric (990-1145 cm^{-1}) and phosphate asymmetric (1190-1275 cm^{-1}) bands for controls and transformed cells using: (a) FTIR-MSP and (b) FTIR- FEWS methods.

Figure 5: Carbohydrate levels calculated as the ratio of the integrated absorbance of the glycogen band at 1045 cm^{-1} / Amide II using: (a) FTIR-MSP and (b) FEWS-FTIR.

Figure 6: Absorbance ratios (FTIR-FEWS / FTIR-MSP) of symmetric and asymmetric bending of CH3 vibration at 1450 and 1400 cm^{-1} (Integration range 1480-1350 cm^{-1}) per

Amide II for the two cell types. The shadowed blue and red bands represent the average value and the standard deviation for the control and the transformed cells respectively.

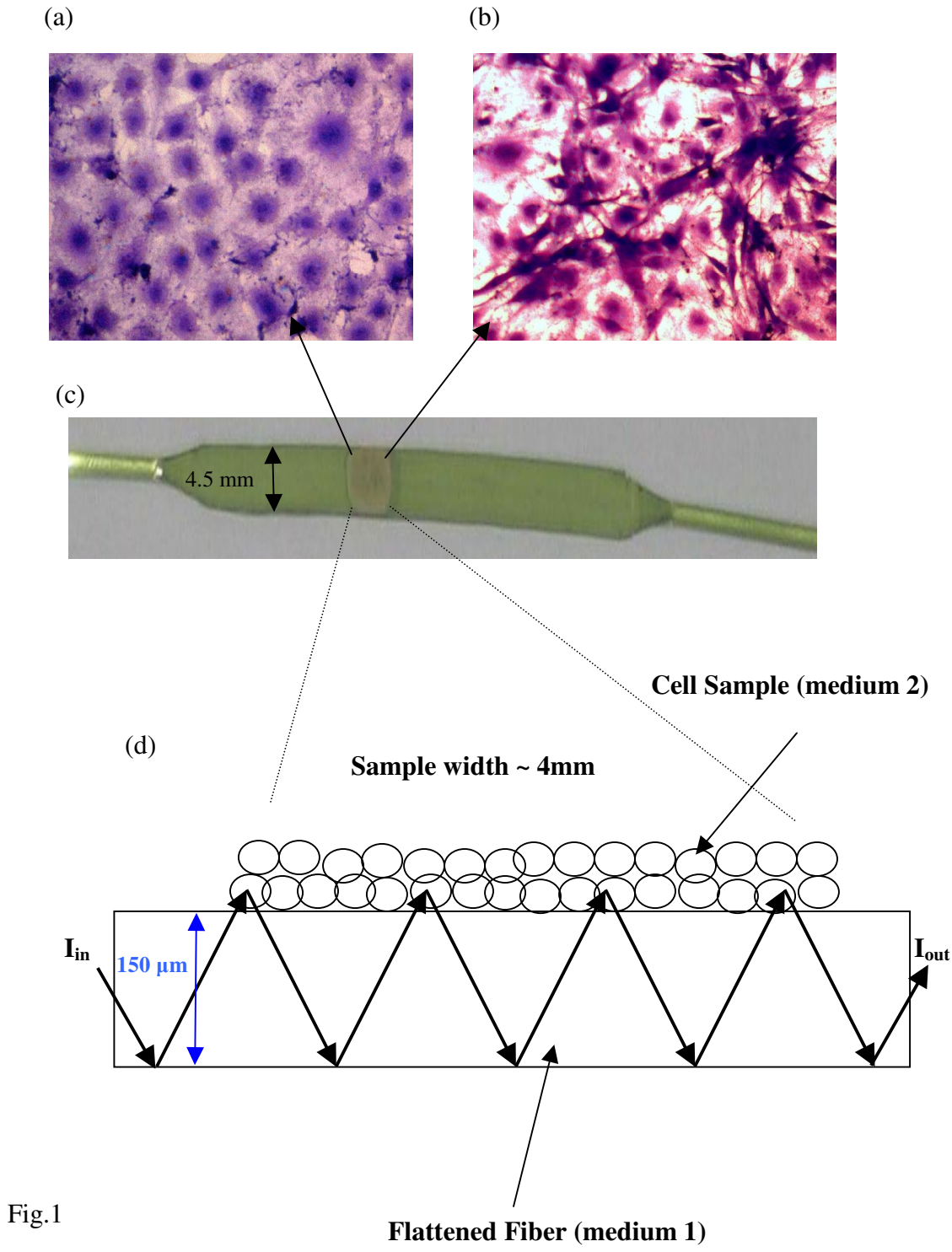
(a)
(b)
(c)
4.5 mm
(d)
Cell Sample (medium 2)
Sample width ~ 4mm
I_{in}
150 µm
I_{out}
Flattened Fiber (medium 1)

Fig.1

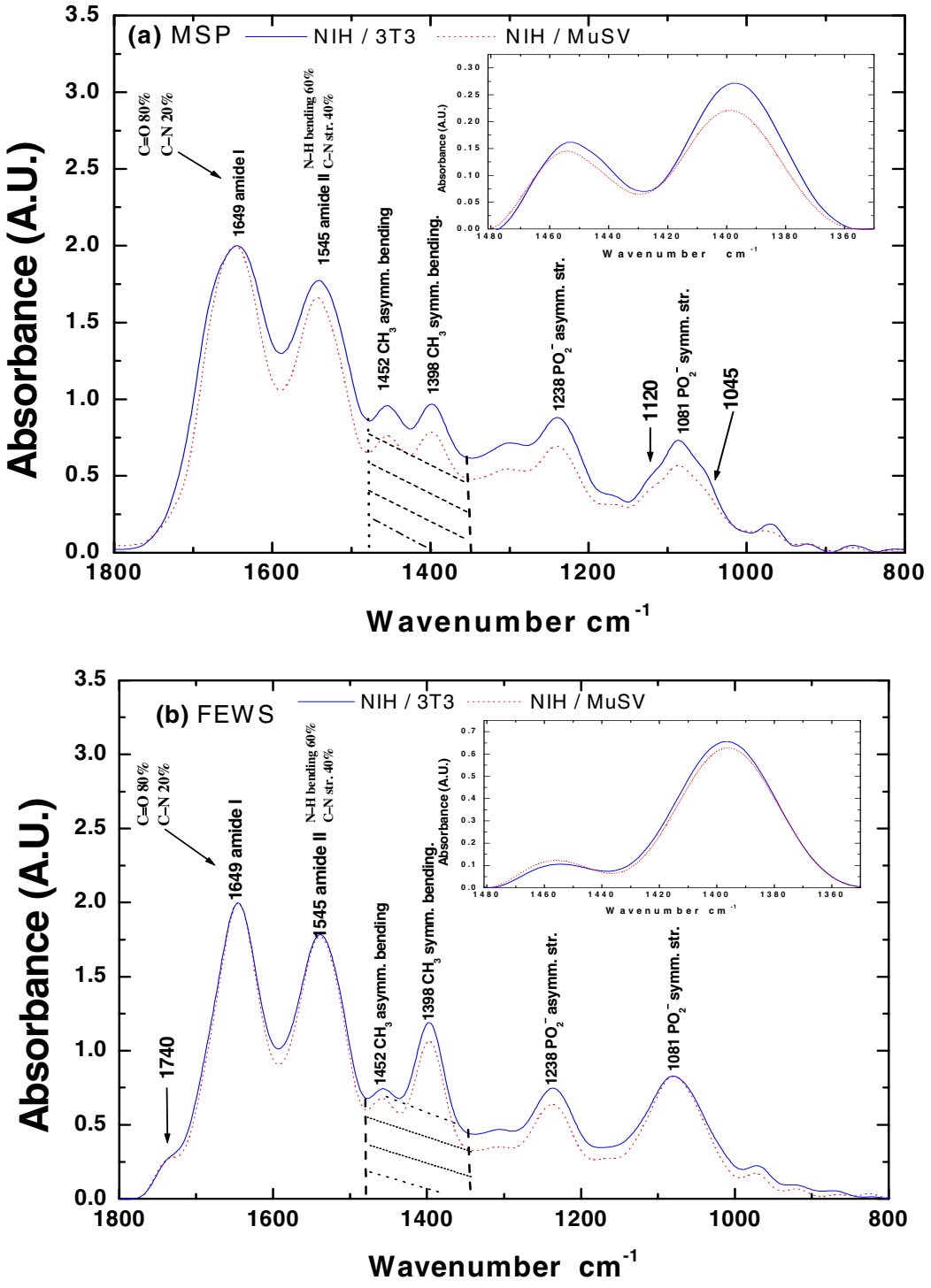
(a) MSP
NIH / 3T3
NIH / MuSV
C=O 80%
C–N 20%
1649 amide I
N–H bending 60%
C–N str. 40%
1545 amide II
1452 CH3 asymm. bending
1398 CH3 symm. bending.
1238 PO2- asymm. str.
1120
1081 PO2- symm. str.
1045
Absorbance (A.U.)
Wavenumber cm-1
(b) FEWS
NIH / 3T3
NIH / MuSV
C=O 80%
C–N 20%
1649 amide I
N–H bending 60%
C–N str. 40%
1545 amide II
1740
1452 CH3 asymm. bending
1398 CH3 symm. bending.
1238 PO2- asymm. str.
1081 PO2- symm. str.
Absorbance (A.U.)
Wavenumber cm-1

Fig. 2

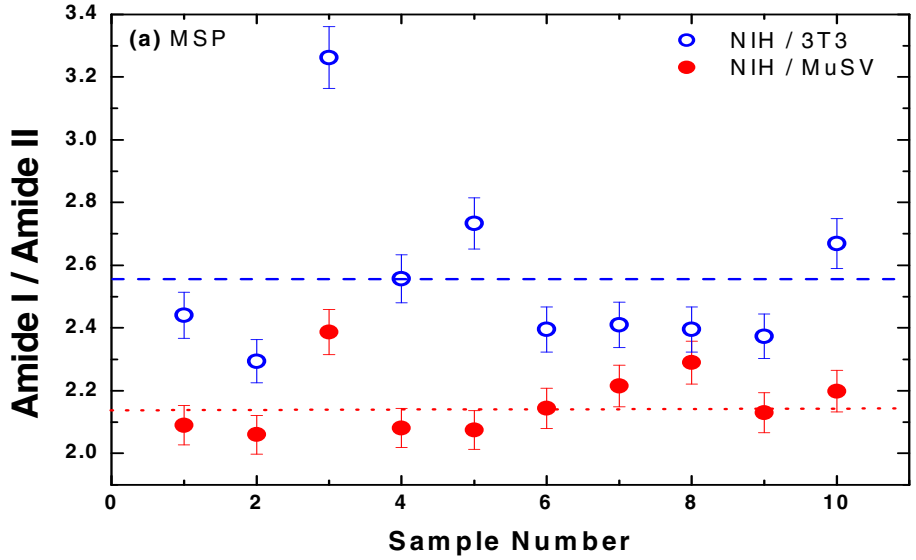
(a) MSP
NIH / 3T3
NIH / MuSV
Amide I / Amide II
Sample Number

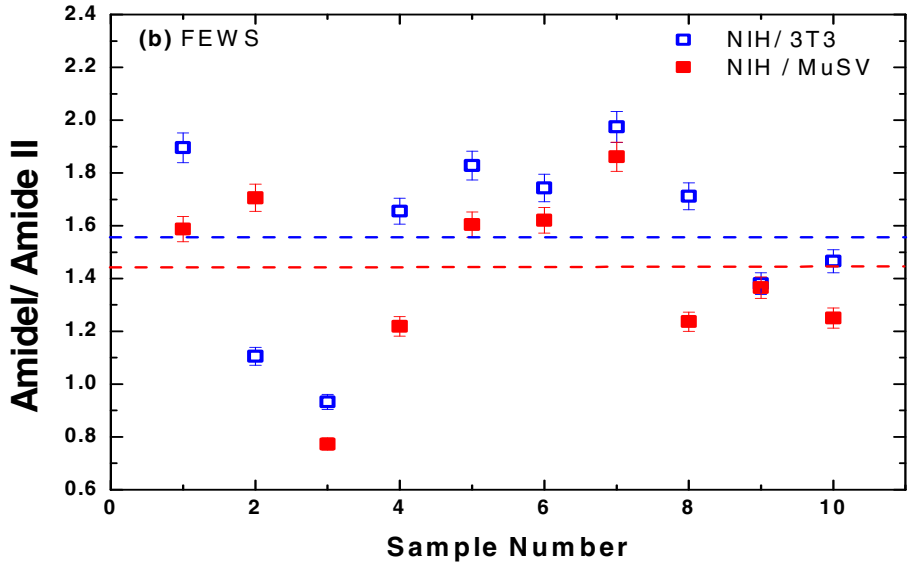
(b) FEWS
NIH/ 3T3
NIH / MuSV
Amidel/ Amide II
Sample Number

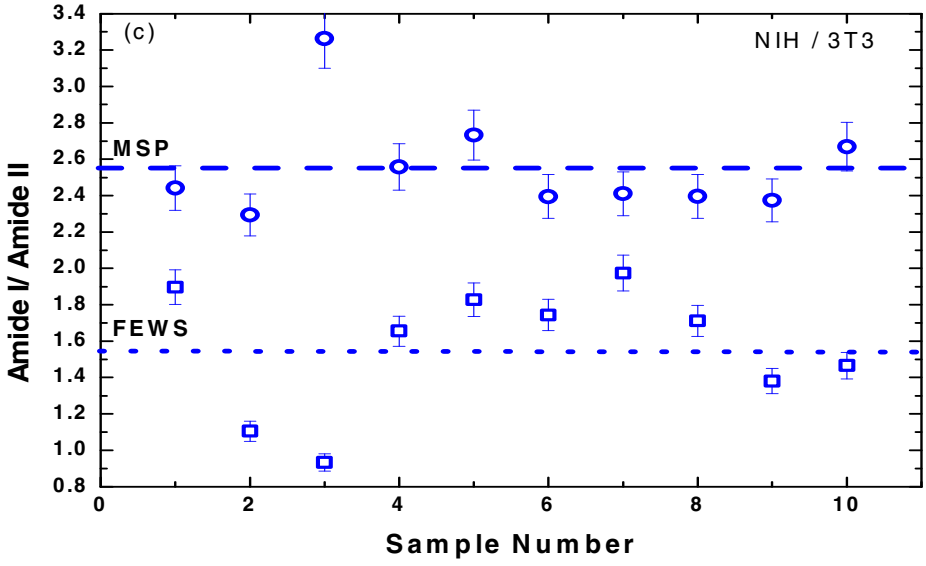
(c)
NIH / 3T3
MSP
FEWS
Amide I/ Amide II
Sample Number

Fig. 3

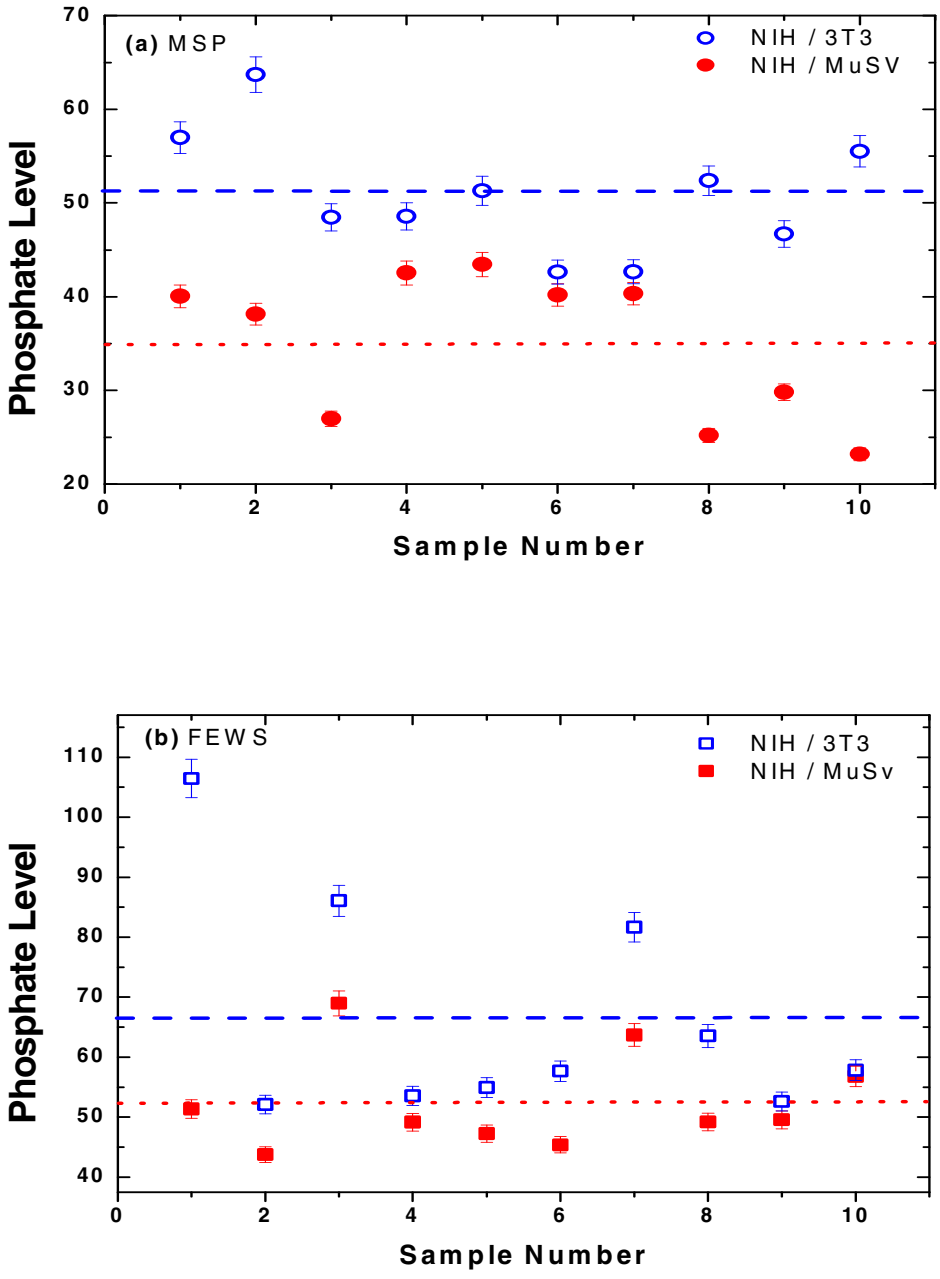
(a) MSP
NIH / 3T3
NIH / MuSV
Phosphate Level
Sample Number
70
60
50
40
30
20
0
2
4
6
8
10
(b) FEWS
NIH / 3T3
NIH / MuSv
Phosphate Level
Sample Number
110
100
90
80
70
60
50
40
0
2
4
6
8
10

Fig. 4

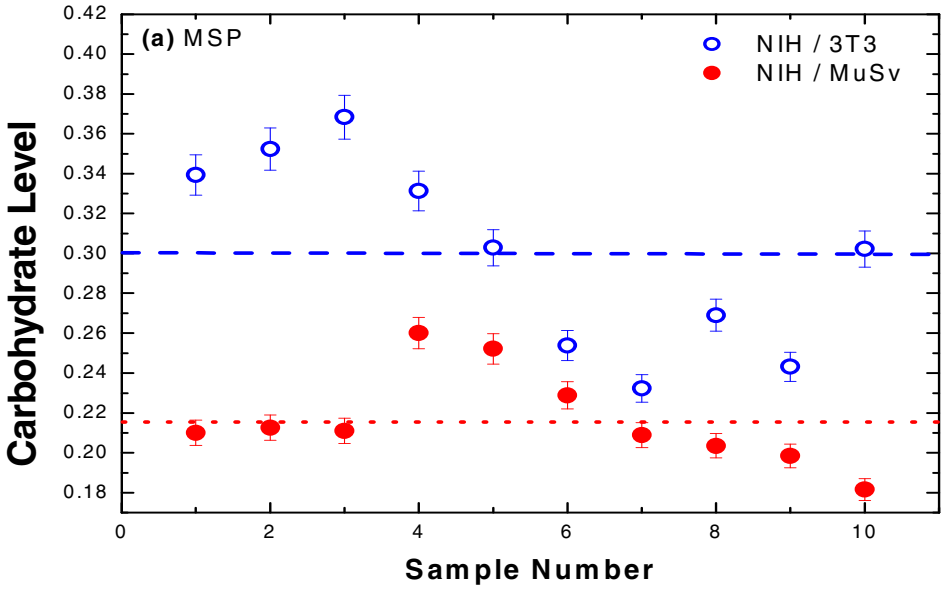
(a) MSP
NIH / 3T3
NIH / MuSv
Carbohydrate Level
Sample Number
0.42
0.40
0.38
0.36
0.34
0.32
0.30
0.28
0.26
0.24
0.22
0.20
0.18
0
2
4
6
8
10

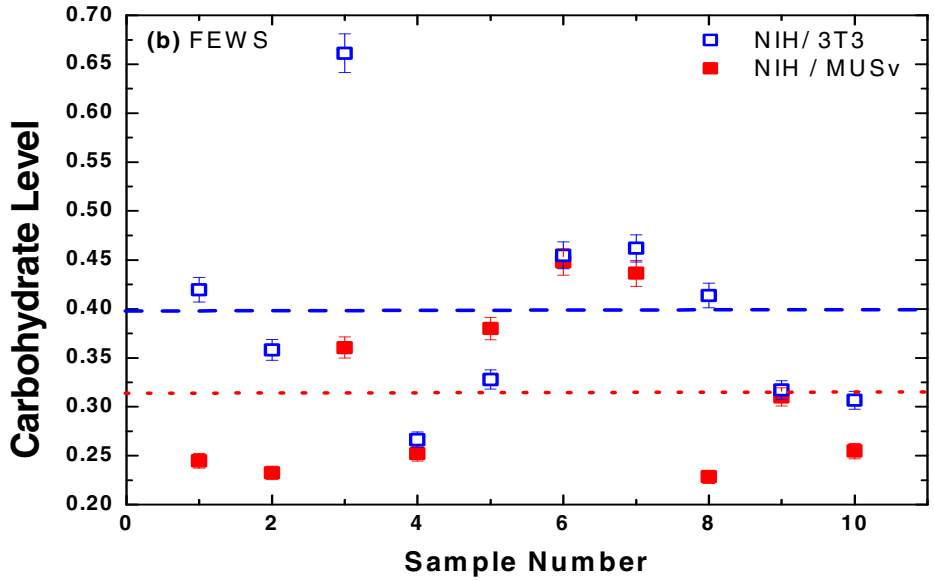
(b) FEWS
NIH/ 3T3
NIH / MUSv
Carbohydrate Level
Sample Number
0.70
0.65
0.60
0.55
0.50
0.45
0.40
0.35
0.30
0.25
0.20
0
2
4
6
8
10

Fig. 5

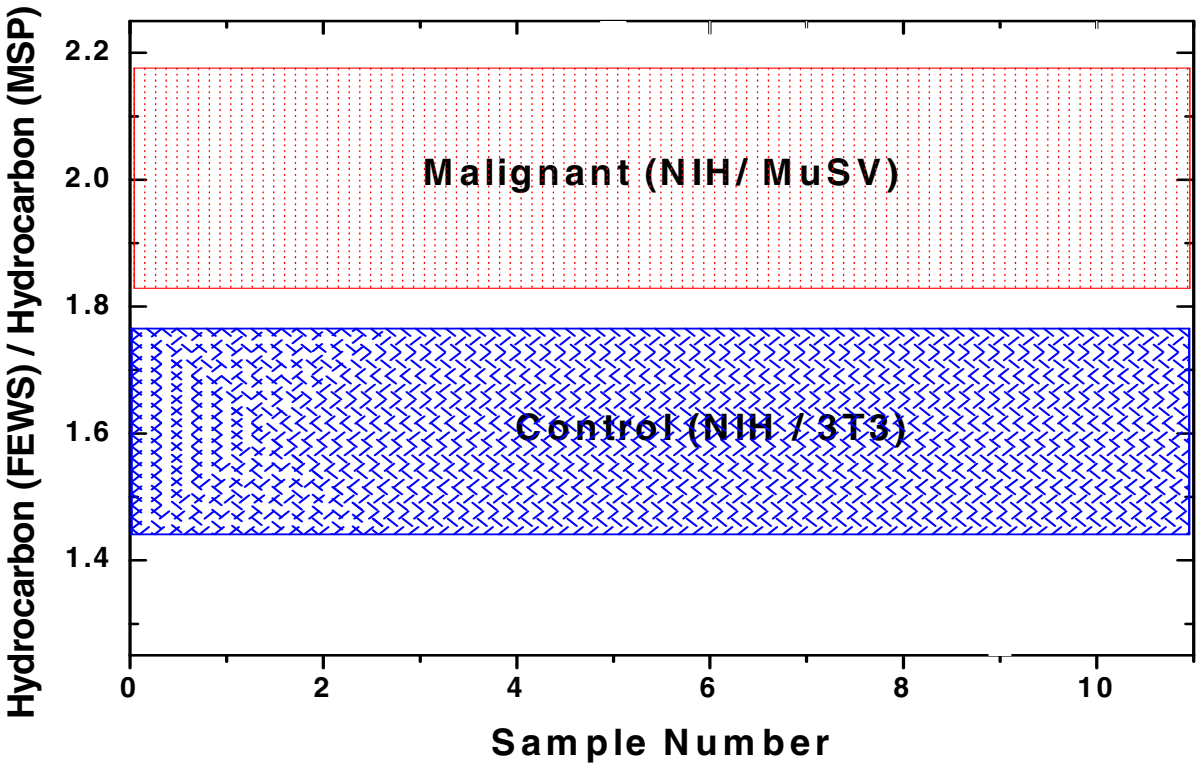
Hydrocarbon (FEWS) / Hydrocarbon (MSP)
2.2
2.0
1.8
1.6
1.4
Malignant (NIH/ MuSV)
Control (NIH / 3T3)
0
2
4
6
8
10
Sample Number

Fig. 6

Table 1: t-Test statistical analysis of the biomarkers derived from the microscopic transmission spectra (MSP) and the flattened fiber internal reflection spectra (FEWS).

Biomarker	**FTIR-MSP**				**FTIR- FEWS**			
	Mean Value		***t-value***	***p-value***	Mean Value		***t-value***	p-value
	NIH/3T3	NIH/MuSV			NIH/3T3	NIH/MuSV		
AmideI/ AmideII	2.55±0.09	2.16±0.03	4.009	0.0008	1.57±0.11	1.42±0.10	0.9920	0.3340
Phosph. Level	50.9±2.1	35.0±2.5	**4.935**	**0.0001**	66.6±5.8	52.5±2.6	**2.2100**	**0.0400**
Carbo. Level	0.299±0.015	0.216±0.007	**4.8650**	**0.0001**	0.398±0.035	0.314±0.026	**1.8710**	**0.0770**
RNA/DNA (1244/1230)	1.019±0.003	1.037±0.003	2. 3312	0.0310	0.988±0.015	0.999±0.022	0.6230	0.3900
RNA/DNA (1121/1020)	2.560±0.155	2.449±0.131	0.8556	0.4231	2.190±0.589	2.295±0.393	0.8330	0.1482